




Intraoperative image-guidance during robotic surgery: is there clinical evidence of enhanced patient outcomes?

Stefano Tappero¹ · Giuseppe Fallara² · Francesco Chierigo^{1,3,4,5} · Andrea Micalef^{6,7} · Francesca Ambrosini^{4,5} · Raquel Diaz⁵ · Andrea Dorotei^{8,9} · Edoardo Pompeo¹⁰ · Alessia Limena^{11,12} · Carlo Andrea Bravi^{13,14} · Mattia Longoni^{15,16} · Mattia Luca Piccinelli² · Francesco Barletta^{15,16} · Luigi Albano^{10,17} · Elio Mazzone^{15,16} · Paolo Dell'Oglio^{1,18,19} 

Received: 19 December 2023 / Accepted: 25 March 2024 / Published online: 12 April 2024
© The Author(s), under exclusive licence to Springer-Verlag GmbH Germany, part of Springer Nature 2024

Abstract

Background To date, the benefit of image guidance during robot-assisted surgery (IGS) is an object of debate. The current study aims to address the quality of the contemporary body of literature concerning IGS in robotic surgery throughout different surgical specialties.

Methods A systematic review of all English-language articles on IGS, from January 2013 to March 2023, was conducted using PubMed, Cochrane library's Central, EMBASE, MEDLINE, and Scopus databases. Comparative studies that tested performance of IGS vs control were included for the quantitative synthesis, which addressed outcomes analyzed in at least three studies: operative time, length of stay, blood loss, surgical margins, complications, number of nodal retrievals, metastatic nodes, ischemia time, and renal function loss. Bias-corrected ratio of means (ROM) and bias-corrected odds ratio (OR) compared continuous and dichotomous variables, respectively. Subgroup analyses according to guidance type (i.e., 3D virtual reality vs ultrasound vs near-infrared fluorescence) were performed.

Results Twenty-nine studies, based on 11 surgical procedures of three specialties (general surgery, gynecology, urology), were included in the quantitative synthesis. IGS was associated with 12% reduction in length of stay (ROM 0.88; $p=0.03$) and 13% reduction in blood loss (ROM 0.87; $p=0.03$) but did not affect operative time (ROM 1.00; $p=0.9$), or complications (OR 0.93; $p=0.4$). IGS was associated with an estimated 44% increase in mean number of removed nodes (ROM 1.44; $p<0.001$), and a significantly higher rate of metastatic nodal disease (OR 1.82; $p<0.001$), as well as a significantly lower rate of positive surgical margins (OR 0.62; $p<0.001$). In nephron sparing surgery, IGS significantly decreased renal function loss (ROM 0.37; $p=0.002$).

Conclusions Robot-assisted surgery benefits from image guidance, especially in terms of pathologic outcomes, namely higher detection of metastatic nodes and lower surgical margins. Moreover, IGS enhances renal function preservation and lowers surgical blood loss.

Keywords Augmented reality · Fluorescence · Intraoperative guidance · Robotic surgery · Tracers · Ultrasound · Virtual reality · 3D models

Introduction

Currently, robot-assisted systems allow the performance of the majority of complex surgeries, traditionally conducted with either an open or a laparoscopic approach. Surgical

experience is maximally enhanced by utmost movement precision, excellent ergonomics, and minimal patient cosmetic consequences [1, 2].

To date, multiple robotic systems have emerged as innovative solutions in the field of minimally invasive surgery and numerous technical refinements have been progressively implemented to the daily robotic practice [2]. Among the latter, intraoperative image guidance emerges as needful support during robotic procedures as, for instance, in the distinction of malignant vs benign tissues, and in the

ST and GF share first authorship.

EM and PDO share last authorship.

Extended author information available on the last page of the article

identification of specific anatomic structures (e.g., blood or lymphatic vessels, lymph nodes, or glands) [3–6]. Image guidance includes a heterogeneous variety of tools, among which near-infrared fluorescence (NIRF) [7], intraoperative ultrasound (IOUS) [8], and augmented reality (AR) [9, 10] represent some of the most widespread.

Fluorophore-based NIRF (e.g., indocyanine green [ICG]-NIRF) provides deep photon penetration (near infrared region, between 650 and 900 nm), thus magnifying optical contrast. NIRF tracers are not visible using white light and their use does not obscure the routine surgical field. Therefore, dedicated NIRF cameras allow to instantaneously switch from white light vision to NIRF vision upon request of the operator, and vice versa [11].

When the proper understanding of anatomy is a matter of crucial relevance, either, for example, concerning the relationship of a tumor with the surrounding healthy parenchyma, or the stream of arteries and veins, IOUS and AR provide further assistance. These types of image guidance increase the meticulousness of surgical gestures, mainly enhancing precision in tumor resection, as well as vascular isolation and clamping. These are all aspects involved in improving patient surgical outcomes, as intraoperative adverse events, surgical margins, ischemia time, and overall procedural time, among others [12].

The current literature regarding image-guided surgery (IGS) is flourishing [13–15]. However, the real impact of such heterogeneous technologies applied to different surgical fields on everyday practice has never been deeply addressed. In consequence, the real additional benefit of IGS during robot-assisted procedures remains an object of debate, and the magnitude of such benefit may be different according to the various surgical fields where IGS is used.

The objective of the current study consists in assessing the quality of the contemporary body of literature concerning IGS in robotic surgery throughout different surgical specialties. Additionally, the current study aims to provide meta-analytic data concerning the actual surgical benefits of the adoption of IGS during robotic procedures.

Materials and methods

Study identification and evaluation

A systematic review of the literature was conducted using the PubMed, Cochrane Central Register of Controlled Trials (CENTRAL), EMBASE, MEDLINE, and Scopus databases. We searched from inception of the databases up to March 1, 2023. All the references for key reviews on IGS were also screened. Keywords used for the research were as follows: “((robotic surgery OR robot-assisted) AND (image-guided surgery OR radio-guided surgery OR molecular imaging

OR molecular trac* OR hybrid trac* OR bimodal trac* OR fluorescence imaging OR magnetic particles OR ultrasound guidance OR augmented reality OR virtual reality OR 3D) AND (staging accuracy OR diagnosis OR metastases OR complications OR oncological outcomes OR functional outcomes OR recurrence OR survival OR mortality).” This systematic review is reported in accordance with the Preferred Reporting Items for Systematic Reviews and Meta-analyses Protocols (PRISMA-P) guidelines [16] and is registered within the international prospective registry of systematic reviews (PROSPERO, CRD42023480670).

Initial screening, eligibility criteria, and risk of bias assessment

After identifying all eligible studies, eleven independent reviewers screened all titles and abstracts (or full text, for further clarification) for inclusion in the study. Literature reviews, editorials, comments, and studies that did not answer the review question were excluded at the eligibility evaluation (Fig. 1). Also, studies including small sample size (less than ten patients) were excluded. Lastly, only comparative studies that tested performance of an intraoperative guidance vs control were included for the final quantitative synthesis, yielding a final cohort of 29 assessable studies. Disagreements regarding eligibility were resolved by discussion with third parties (EM, PD) until consensus was reached.

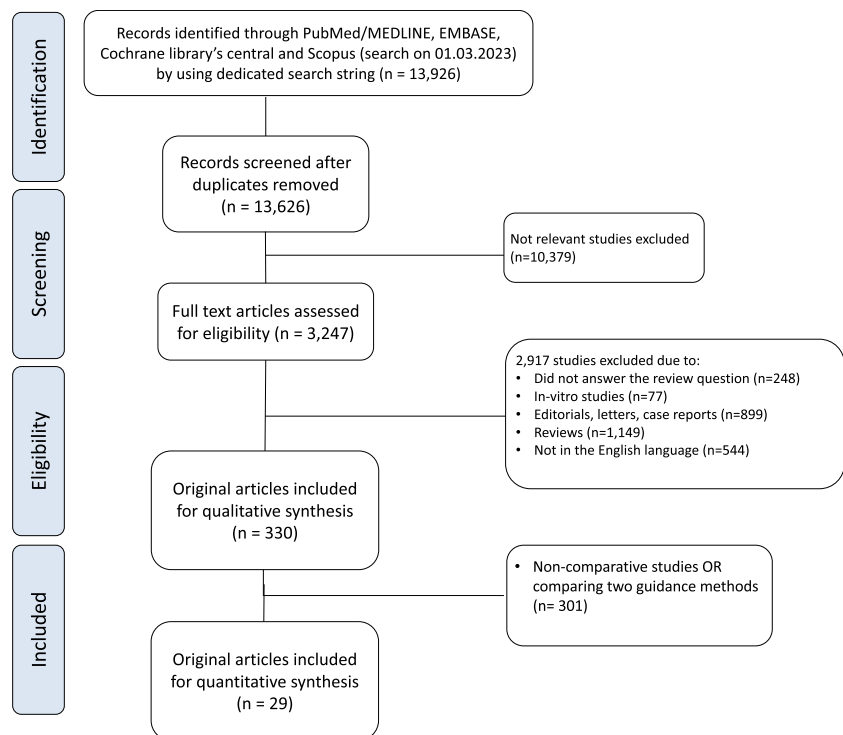
Methodological quality of the included studies was graded using modified Risk Of Bias in Non-Randomized Studies-of Intervention (ROBINS-I) checklist [17]. Three investigators (AM, FC, ST) independently assessed the risk of bias for all studies. In case of disagreements, a discussion with an additional experienced investigator (EM) was carried out.

Intervention and comparison arms

For meta-analytic evaluation, the intraoperative surgical guidance was considered the experimental arm. The group which received standard surgery represented the comparison arm (Table 1). Of the 29 assessable studies, 18 used ICG-NIRF [18–35], nine used 3D/VR guidance [36–44], and two used US guidance [45, 46].

- ICG-NIRF

Freshly prepared ICG is diluted to 2.5 mg/ml with a maximum dosage of 2 mg/kg [21]. After the administration of the dye, the light can be switched to NIRF. The pass of ICG can be observed in the surgical field of interest (i.e., kidney [18–21], lymph nodes [23–27], ureteral

Fig. 1 PRISMA flow diagram

anastomosis[22], uterus [28], thyroid [29, 30, 32], stomach [33–35], rectal sphincter [31]) after approximately 2 min. An exact discrimination between vascularized and de-vascularized areas can be achieved.

ICG can also be used for Sentinel Node Biopsy procedure. In this case, free-ICG (5 mg in 2 mL of sterile water) or combined with ^{99m}Tc -nanocolloid (0.5 mg of albumin, 0.25 mg of ICG, and 240 MBq of ^{99m}Tc in 2 mL of saline) can be injected in the organ of interested (i.e., prostate [47]) and used for sentinel node biopsy via lymphatic mapping.

- 3D/VR guidance

The three-dimensional virtual model of the anatomy of interest (i.e., kidney [36, 38–40, 42], prostate [41–43]) is originated from computed tomography or magnetic resonance images, using a specific software among those nowadays available on the market. Typically, a rendered colored virtual-segmented 3D model can be rotated in all dimensions, and each extracted volume (e.g., tumor, pyelo-caliceal system, renal cortex, seminal vesicles) can be made opaque, translucent, or hidden, separately.

- US

A drop-in US probe inserted by the table assistant and maneuvered by the console surgeon allows real-time visualization of the surgical target (e.g., renal tumor, edge between

healthy parenchyma and tumor [45], vascular structures, ureter, perineal pelvic floor [46]).

Outcomes definition

For pooled meta-analysis, we evaluated outcomes that were assessed in at least three studies. Specifically, the following outcomes were assessed among studies of all specialties considered: operative time, length of stay (LOS), estimated blood loss (EBL), surgical margins, postoperative complication rate, overall number of nodal retrievals, number of positive nodes identified, ischemia time, and estimated reduction of glomerular function (eGFR). Additional single-studies outcomes were described within qualitative synthesis and reported in Table 1.

Data synthesis and statistical analysis

Data not suitable for meta-analytic evaluation was presented in a narrative fashion (qualitative analysis). Reported results for continuous outcomes were pooled using bias-corrected ratio of means (ROM) according to previous established methodology [48, 49]. Thus, the bias-corrected odds ratio (OR) were used to compare dichotomous variables, respectively. All results were reported with 95% confidence intervals. Pre-planned subgroups analyses were performed in studies after stratification according to the type of intraoperative guidance (3D/VR vs UltraSound vs NIRF-ICG vs Hybrid Nanocolloid vs Carbon nanoparticles).

Table 1 Characteristics of studies included in the quantitative meta-analysis

Field of research	Reference	Study period	Study design	Study origin	Surgery	Image guidance	Cases/controls, n	Surgical outcomes	Study-specific outcomes
1. Urology, kidney	Lanchon	2015–2016	PRS; PC; SC	The Netherlands	RAPN	NIRF with ICG	25/25	OT ^a : 123 vs 119 min LOS ^a : 5 vs 5 days EBL ^a : 105 vs 95 mL	Ischemia time ^a : 14 vs 15 min Loss of eGFR ^a : –2 vs –16%
2. Urology, kidney	Borofsky	2011	RTP; PC; MI	USA	RAPN	NIRF with ICG	34/27	OT ^b : 256 vs 212 min EBL ^b : 207 vs 249 mL Complications: 26 vs 30%	Loss of eGFR: –1.8 vs –15%
3. Urology, kidney	Mattevi	2015–2017	RTP; PC; SC	Italy	RAPN	NIRF with ICG	20/42	OT ^a : 190 vs 206 min LOS ^a : 5 vs 5 days EBL ^a : 170 vs 200 mL Complications: 10 vs 38%	Ischemia time ^a : 24 vs 24 min Loss of eGFR: –5.5 vs –21.5%
4. Urology, kidney	Shirk	–	RTP; PC; SC	USA	RAPN	3D virtual reality	30/30	OT ^a : 175 vs 185 min EBL ^a : 125 vs 150 mL LOS > 2 days: 53 vs 73%	Ischemia time ^a : 12.5 vs 15 min
5. Urology, kidney	Kobayashi	2013–2018	RTP; PSM; SC	Japan	RAPN	3D virtual reality	42/42	Complications: 14.3 vs 7.1%	Ischemia time ^a : 14 vs 16 min Surgical margins: 0 vs 2.4%
6. Urology, kidney	Sun	2016–2018	RTP; PC; SC	China	RAPN	IOUS	38/20	OT ^b : 201 vs 190 min LOS ^b : 8 vs 8 days EBL ^b : 145 vs 258 mL Complications: 15.8 vs 35%	Loss of eGFR: –6.4 vs –9.9% Ischemia time ^b : 20 vs 26 min Surgical margins: 7.9 vs 15% Trifecta rate (MIC): 58 vs 30%
7. Urology, kidney	Harke	2013	RTP; PC; SC	Germany	RAPN	NIRF with ICG	15/15	OT ^b : 154 vs 162 min EBL ^b : 300 vs 228 mL Complications: 13 vs 13%	Ischemia time ^b : 11.5 vs 12 min

Table 1 (continued)

Field of research	Reference	Study period	Study design	Study origin	Surgery	Image guidance	Cases/controls, n	Surgical outcomes	Study-specific outcomes
8. Urology, kidney	Michiels	2016–2020	RTP; PSM; MI	France	RAPN	3D virtual reality	157/157	OT ^a : 172 vs 119 min LOS ^a : 1 vs 2 days EBL ^a : 200 vs 200 mL Complications: 11.5 vs 14%	Ischemia time ^a : 28 vs 16 min Surgical margins: 4.5 vs 5.7% Loss of eGFR: –7.8 vs –11.8% Trifecta rate: 55.8 vs 45.1%
9. Urology, kidney	Shirk	2017–2018	RCT; MI	United States	RAPN	3D virtual reality	44/48	OT ^a : 163 vs 174 min LOS > 2 days: 9 vs 15% EBL ^a : 100 vs 100 mL	Ischemia time ^a : 18 vs 18 min
10. Urology, kidney	Cheng	2018–2020	RTP; PC; SC	China	Robot-assisted pyeloplasty	3D virtual reality	16/22	OT ^a : 128 vs 132 min EBL ^b : 20 vs 30 mL Complications: 0 vs 5%	Success rate: 100 vs 91%
11. Urology, bladder	Ahmadi	2014–2017	RTP; PC; SC	USA	RARC	NIRF with ICG	47/132	OT ^a : 480 vs 430 min LOS ^a : 5 vs 5 days EBL ^a : 200 vs 200 mL Complications: 62 vs 71%	Uretero-enteric stricture rate: 0 vs 10.6%
12. Urology, prostate	Grivas	2006–2016	RTP; PC; SC	The Netherlands	RARP	NIRF with ICG	184/736	–	Biochemical recurrence: 19.5 vs 20.1% Lymph nodes detection ^a : 14 vs 9
13. Urology, prostate	Harke	2014–2015	RCT; SC	Germany	RARP	NIRF with ICG	60/60	Complications: 5 vs 1.6%	Surgical margins: 12 vs 12% Lymph nodes detection ^a : 25 vs 17 Positive lymph nodes detection: 15 vs 10%
14. Urology, prostate	Bianchi	2019	RTP; PSM; SC	Italy	RARP	3D virtual reality	20/20	OT ^b : 216 vs 209 min EBL ^b : 200 vs 183 mL LOS ^a : 3 vs 3 days Complications: 10 vs 5%	Surgical margins: 15 vs 20%

Table 1 (continued)

Field of research	Reference	Study period	Study design	Study origin	Surgery	Image guidance	Cases/controls, n	Surgical outcomes	Study-specific outcomes
15. Urology, prostate	Shirk	2019–2020	RCT, MI	USA	RARP	3D virtual reality	41/51		Surgical margins: 10 vs 16% Urinary continence at 6 months: 0.9 vs 1.4 pads per day SHIM score at 6 months ^b : 18.7 vs 18.6 PSA persistency: 3 vs 11% Surgical margins: 25 vs 35%
16. Urology, prostate	Checceucci	2016–2020	PRS; PC; SC	Italy	RARP	3D virtual reality	800/800	OT ^b : 113 vs 118 min Complications: 5.6 vs 4.8%	
17. Urology, prostate	Mazzone	2006–2019	RTP; PC; SC	The Netherlands	RARP	NIRF with ICG alone* NIRF with ICG- ^{99m} Tc-nanocolloid ^o	161/1168* 351/1168 ^o	OT ^a : 111 vs 115 min* 121 vs 115 min ^o Complications: 29 vs 34%* 39 vs 34% ^o	Surgical margins: 37 vs 39%* 32 vs 39% ^o Biochemical recurrence: 61 vs 45%* 42 vs 45% ^o Lymph nodes detection ^a : 20 vs 11* 17 vs 11 ^o Positive lymph nodes detection: 36 vs 19%* 28 vs 19% ^o Progression free survival: 73 vs 67%* 67 vs 67% ^o
18. Urology, prostate	Porpiglia	2018	PRS; PC; SC	Italy	RARP	3D virtual reality	20/20	OT ^b : 140 vs 118 min LOS ^a : 5.3 vs 5.6 days EBL ^b : 240 vs 230 mL Complications: 10 vs 10%	Surgical margins: 25 vs 35% Capsular involvement identification: 100 vs 47%
19. Urology, penis	Yuan	2018–2020	RTP; PC; SC	China	Robot-assisted inguinal lymph node dissection	NIRF with ICG	10/16	OT ^a : 100 vs 106 min LOS ^a : 5.5 vs 6 days EBL ^a : 70 vs 88 mL Complications: 20 vs 25%	Lymph nodes detection ^a : 29.5 vs 25 Positive lymph nodes detection: 20 vs 31%

Table 1 (continued)

Field of research	Reference	Study period	Study design	Study origin	Surgery	Image guidance	Cases/controls, n	Surgical outcomes	Study-specific outcomes
20. Gynecology, uterus	Holloway	2006–2013	RTP; PC; SC	USA	Pelvic and aortic robot-assisted lymph node dissection	NIRF with ICG	119/661	OT ^b : 158 vs 155 min LOS ^b : 18 vs 17 days EBL ^b : 120 vs 105 mL Complications: 7 vs 13%	Lymph nodes detection ^b : 35.4 vs 27.8 Positive lymph nodes detection: 30.3 vs 14.7%
21. Gynecology, uterus	Davila	2016–2019	RTP; PC; MI	USA	Robot-assisted sacrocervicopexy	IOUS	15/15	OT ^b : 170 vs 135 min LOS ^b : 18 vs 17 days EBL ^b : 120 vs 105 mL Complications: 7 vs 13%	–
22. Gynecology, uterus	El-Achi	2018–2021	RTP; PC; SC	Australia	Robot-assisted hysterectomy	NIRF with ICG	68/14	OT ^b : 132 vs 171 min LOS ^b : 1.5 vs 1.4 days EBL ^b : 53 vs 212 mL Complications: 0 vs 7%	–
23. General surgery, thyroid	Yu	2013–2015	RTP; PSM; SC	Korea	Robot-assisted thyroidectomy	NIRF with ICG	22/44	–	Parathyroid glands preservation: 0 vs 16%
24. General surgery, thyroid	Ouyang	2020–2021	RTP; PC; SC	China	Robot-assisted thyroidectomy	NIRF with ICG	34/47	OT ^b : 89 vs 81 min LOS ^b : 2.6 vs 2.9 days EBL ^b : 12.9 vs 13.3 mL	Parathyroid glands preservation ^b : 3.1 vs 2.7
25. General surgery, thyroid	Kim	2015–2016	PRS; PC; SC	Korea	Robot-assisted thyroidectomy	NIRF with ICG	55/55	OT ^b : 162 vs 165 min LOS ^b : 3.6 vs 3.9 days	Lymph nodes detection ^b : 7 vs 4.8 Positive lymph nodes detection ^b : 1 vs 0.4
26. General surgery, stomach	Lan	2011–2016	PRS; PC; SC	Taiwan	Robot-assisted gastrectomy	NIRF with ICG	14/65	OT ^b : 327 vs 349 min LOS ^b : 10.1 vs 11.9 days EBL ^b : 75.7 vs 78.3 mL Complications: 7.1 vs 12.3%	Lymph nodes detection ^b : 35.8 vs 30 Positive lymph nodes detection: 43 vs 34%
27. General surgery, stomach	Cianchi	2014–2018	RTP; PSM; SC	Italy	Robot-assisted gastrectomy	NIRF with ICG	37/37	OT ^b : 321 vs 293 min LOS ^b : 10.9 vs 10.0 days Complications: 13.5 vs 13.5%	–

Table 1 (continued)

Field of research	Reference	Study period	Study design	Study origin	Surgery	Image guidance	Cases/controls, n	Surgical outcomes	Study-specific outcomes
28. General surgery, stomach	Tian	2019–2020	RTP; PC; SC	China	Robot-assisted gastrectomy	NIRF with ICG NIRF with CNSI	27/32* 34/32°	OT ^b : 230 vs 239 min* 228 vs 239 min° EBL ^b : 40 vs 45 mL* 38 vs 45 mL°	Lymph nodes detection ^b : 39.2 vs 35.3* 48.4 vs 35.3° Positive lymph nodes detection: 4.6 vs 5.9%* 5.0 vs 5.9%°
29. General surgery, rectum	Kim	2010–2016	RTP; PC; SC	Korea	Robot-assisted rectal sphincter saving surgeries	NIRF with ICG	310/347	OT ^b : 177 vs 197 min Complications: 10.3 vs 15.3%	Anastomotic leakage rate: 0.6 vs 5.2% Anastomotic stricture rate: 3.5 vs 2.6%

RTP retrospective, PRS prospective, RCT randomized clinical trial, PC paired cohort, PSM propensity score matching, MI multi-institutional, SC single-center, RAPN robot-assisted partial nephrectomy, NIRF near-infrared fluorescence imaging, ICG indocyanine green, OT operative time, LOS length of stay, EBL estimated blood loss, eGFR estimated glomerular filtrate rate, RARP robot-assisted radical prostatectomy, RARC robot-assisted radical cystectomy, IOUS intra-operative ultrasound, CNSI carbon nanoparticle suspension injection, M/C margins, ischemia, complications

^aMedian

^bMean

Heterogeneity between studies was measured using the I^2 statistic [50] and the between-study variance (t^2) from the random-effect analyses. I^2 values > 50% indicate large inconsistency. Unless otherwise indicated, all models have allowed for different effect sizes (random effects). In case of large heterogeneity, random effect models (using the DerSimonian and Laird approach [51]) were prioritized. For the assessment of small study effects and publication bias, values of the ROM or OR were plotted against their standard error in a contour-enhanced funnel plot. The latter bias represents the error in connection with whether a study is published or not depending on the characteristics and result of individual studies [52]. This error is caused because statistically significant study results generally have a higher likelihood of being published. Furthermore, Eggers asymmetry test [53] was used to explore statistically the presence of publication bias. Statistical significance for all analysis was defined as two-sided $p < 0.05$. Statistical analysis was performed with the R software (version 3.6.3; <http://www.r-project.org/>) [54].

Results

Study selection flowchart

Figure 1 shows the flow of studies through the screening process. Overall, 13,626 papers were blindly screened by eleven reviewers (AD, AL, AM, EP, FA, FB, FC, ML, MLP, RD, ST), with 3247 of these records included for further evaluation based on pre-defined eligibility criteria. Of these, 330 studies were considered eligible for final inclusion in qualitative analysis. At this point, final evaluation for the inclusion in the quantitative synthesis was carried out by three reviewers (EM, GF, PD). At the end of the process, 29 manuscripts were included for the quantitative meta-analysis (Table 1).

Study quality and risk of bias

The Supplementary Material Appendix 1a-b summarizes the quality criteria assessed for each study using the ROBINS-I tool. The overall methodological quality of the studies was moderate, with most of the studies having moderate or low risk of bias.

Evidence synthesis

Table 1 summarizes general and design characteristics of the selected studies. Primary analysis included 29 papers for quantitative synthesis. The final screened manuscripts reported outcomes based on 11 different surgical

procedures across the included surgical specialties (general surgery, gynecology and urology). Overall, 18 studies used NIRF with ICG [18–35]. Nine studies used 3D/VR guidance [36–44], while two implemented US guidance [45, 46]. According to the outcomes, 24, 16, and 18 studies assessed operative time [18–22, 25–28, 30–37, 39–41, 43–46], LOS [18, 20, 22, 26, 28, 30, 32–34, 36, 37, 39, 41, 44–46], and EBL [18–22, 26, 28, 30, 33, 35–37, 39–41, 44–46], respectively. Additionally, eight, seven, and nine assessed total number of nodes retrieved [23–27, 32, 33, 35], number of positive nodes [24–27, 32, 33, 35], and rate of surgical margins [9, 24, 25, 38, 39, 41, 42, 44, 45], respectively. Lastly, eight and five tested the impact of IGS on ischemia time [18, 20, 21, 36–39, 45] and eGFR reduction [18–20, 39, 45]. These last concerned nephron-sparing surgery.

In quantitative synthesis testing for operative time, a pooled meta-analysis on 3987 patients was conducted (Fig. 2a), using random-effects models. Overall, intraoperative guidance did not impact operative time (ROM 1.00, 95% CI 0.94; 1.06; $p=0.9$). Funnel plot and Eggers' linear regression estimates (bias 1.36, $p=0.3$) both showed absence for potential publications bias (Supplementary Material Appendix 2). In subgroup analyses according to the guidance used, intraoperative guidance was not associated with different operative time in any of the evaluated groups (Fig. 2b).

In quantitative synthesis testing for LOS, a pooled meta-analysis on 1261 patients was conducted. Overall, at ROM analysis, use of intraoperative guidance was associated with 12% reduction in LOS compared to standard surgery (ROM 0.88, 95% CI 0.77; 0.99; $p=0.03$) (Fig. 3a). Funnel plot and Eggers' linear regression estimates (bias -1.60 , $p=0.4$) recorded absence for potential publications bias (Supplementary Material Appendix 3). When testing type of guidance, LOS reduction was significant only in those studies implementing NIRF-ICG (ROM 0.87, 95% CI 0.80; 0.95; $p=0.02$) (Fig. 3b).

In quantitative synthesis testing for EBL, a pooled meta-analysis on 1496 patients was conducted. Overall, patients treated with intraoperative guided-surgery had lower EBL compared to standard surgery (ROM 0.87, 95% CI 0.77; 0.99, $p=0.03$) (Fig. 4a). Funnel plot and Eggers' linear regression estimates (bias -1.31 , $p=0.4$) demonstrated absence of potential publications bias (Supplementary Material Appendix 4). However, in subgroup analyses, none of the evaluated guidance approach was singularly associated with reduced EBL (Fig. 4b).

In quantitative synthesis testing for number of nodes retrieved, a pooled meta-analysis on 2854 patients was conducted. Overall, patients treated with intraoperative guided-surgery had an estimated 44% increase in mean number of

removed nodes at surgery compared to standard surgery (ROM 1.44, 95% CI 1.18; 1.77, $p<0.001$) (Fig. 5a). Funnel plot and Eggers' linear regression estimates (bias -7.14 , $p=0.03$) demonstrated presence of potential publications bias (Supplementary Material Appendix 5). Subgroups analyses showed that most of the studies included used NIRF-ICG with only one study evaluating the role of hybrid nanocolloid (^{99m}Tc -ICG) (Fig. 5b).

In the quantitative synthesis testing for the rate of metastatic nodal involvement, a pooled meta-analysis on 2920 patients was conducted. Overall, patients who underwent IGS had significantly higher rate of pN1 disease identified (OR 1.82, 95% CI 1.49; 2.21; $p<0.001$ using a common effect model), as confirmed in subgroup analyses according to tracer type (Fig. 6a, b). Funnel plot and Eggers' linear regression estimates (bias -1.10 , $p=0.9$) demonstrated absence of potential publications bias (Supplementary Material Appendix 6).

In the quantitative synthesis testing for the rate of positive surgical margins, a pooled meta-analysis on 1488 patients was conducted. Overall, patients who underwent IGS had significantly lower rate of surgical margins at final pathology compared to standard surgery (OR 0.62, 95% CI 0.46; 0.85; $p<0.001$ using a common effect model) (Fig. 7a, b). Funnel plot and Eggers' linear regression estimates (bias -0.5 , $p=0.1$) demonstrated absence of potential publications bias (Supplementary Material Appendix 7).

In the quantitative synthesis testing for the rate of postoperative complications, a pooled meta-analysis on 4432 patients was conducted. Overall, no differences in rate of postoperative complications were recorded between IGS and standard surgery (OR 0.93, 95% CI 0.79; 1.10; $p=0.4$ using a common effect model) (Fig. 8a). Funnel plot and Eggers' linear regression estimates (bias -0.25 , $p=0.3$) demonstrated absence of potential publications bias (Supplementary Material Appendix 8). The results were consistent even after stratification according to type of guidance used (Fig. 8b).

In quantitative synthesis testing for ischemia time during nephron sparing surgery, a pooled meta-analysis on 745 patients was conducted (Fig. 9a), using random-effects models. Overall, intraoperative guidance did not impact on ischemia time (ROM 0.89, 95% CI 0.76; 1.04; $p=0.5$). Funnel plot and Eggers' linear regression estimates (bias 4.13, $p=0.4$) both showed absence for potential publications bias (Supplementary Material Appendix 9). In subgroup analyses according to tracer used, intraoperative guidance was not associated with different ischemia time in the evaluated group including multiple studies (Fig. 9b).

In quantitative synthesis testing for eGFR reduction after nephron sparing surgery, a pooled meta-analysis on 479

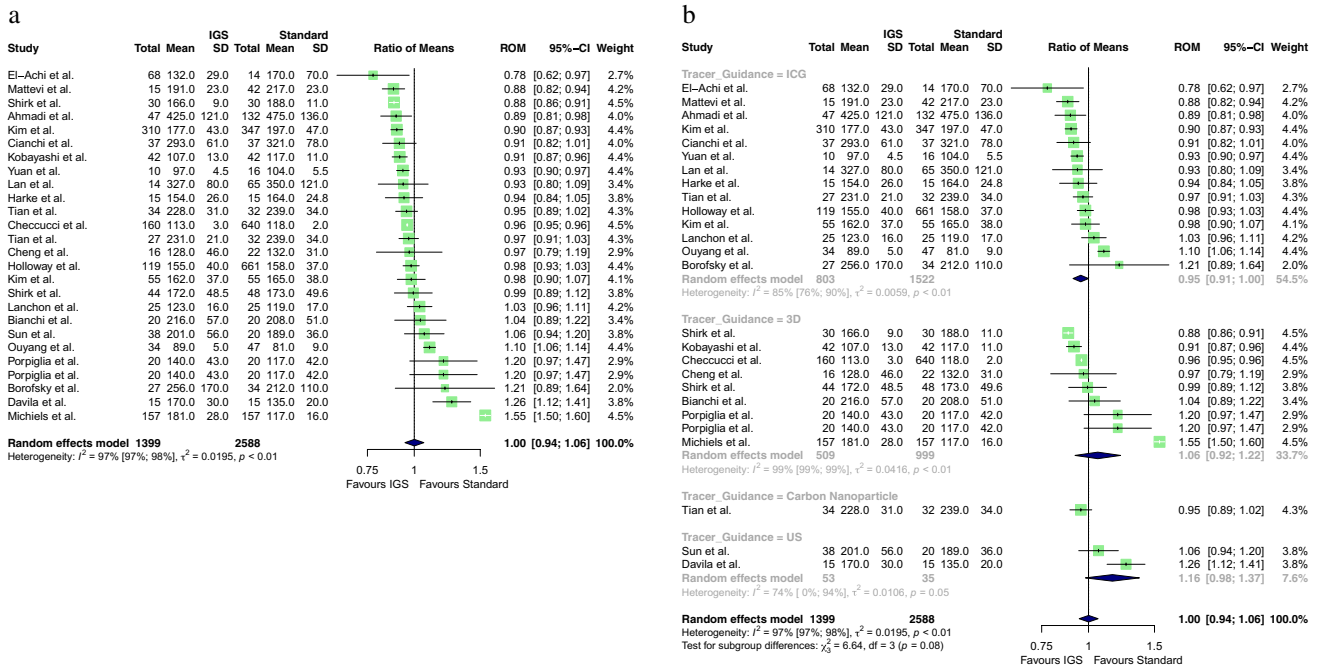


Fig. 2 Quantitative synthesis concerning operative time, **a** regardless of tracer type; **b** according to tracer type

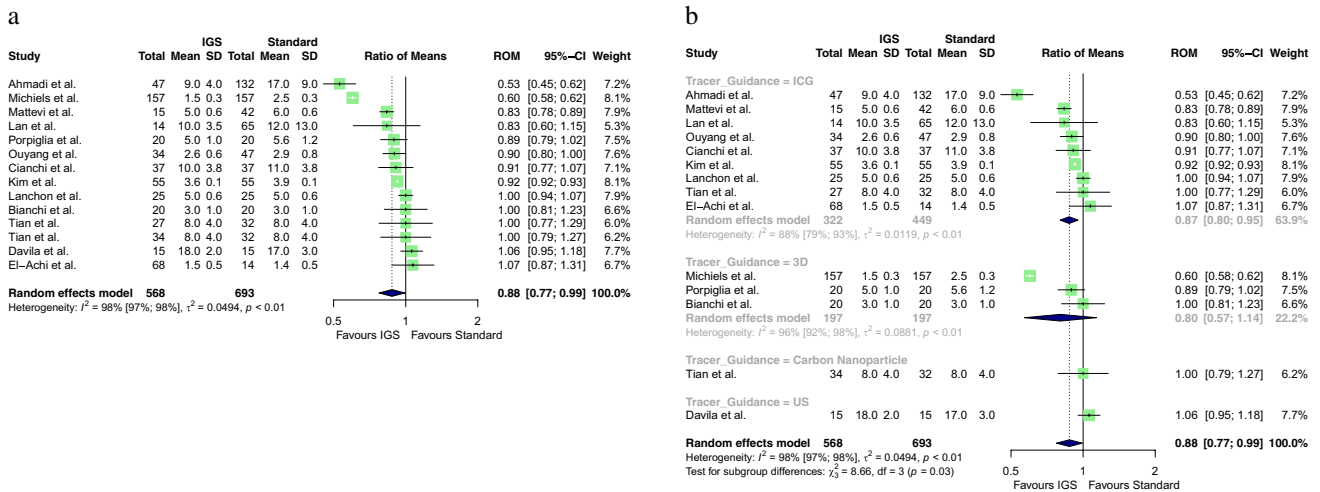


Fig. 3 Quantitative synthesis concerning length of stay, **a** regardless of tracer type; **b** according to tracer type

patients was conducted (Fig. 10a), using random-effects models. Overall, intraoperative guidance was associated with lower magnitude of eGFR reduction (ROM 0.37, 95% CI 0.22; 0.62; $p=0.002$). Funnel plot and Eggers' linear regression estimates (bias -3.92 , $p=0.09$) both showed absence for potential publications bias (Supplementary Material Appendix 10). Subgroup analyses confirmed the efficacy of IGS on eGFR reduction regardless the type of guidance used (Fig. 10b).

Discussion

Imaging is increasingly employed as a tool to enhance the precision of surgical procedures. This comprehensive systematic review and meta-analysis synthesized published evidence on IGS across various surgical specialties and 11 distinct surgical procedures. Despite the inclusion of different IGS modalities, our findings indicate that the utilization of IGS led to significant improvements in several

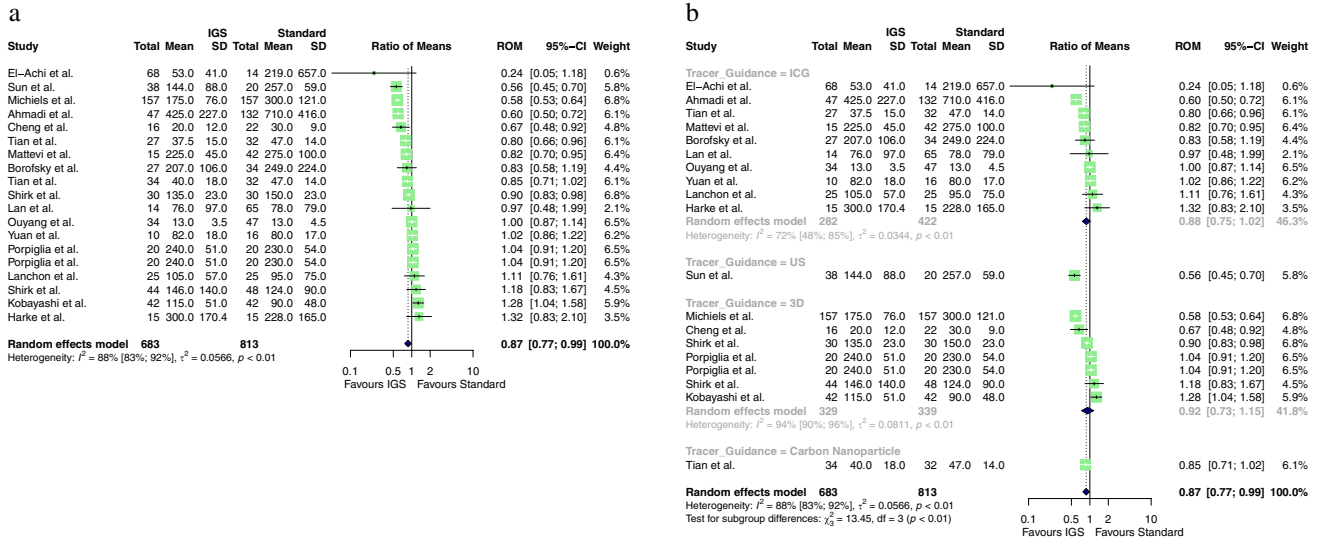


Fig. 4 Quantitative synthesis concerning estimated blood loss, **a** regardless of tracer type; **b** according to tracer type

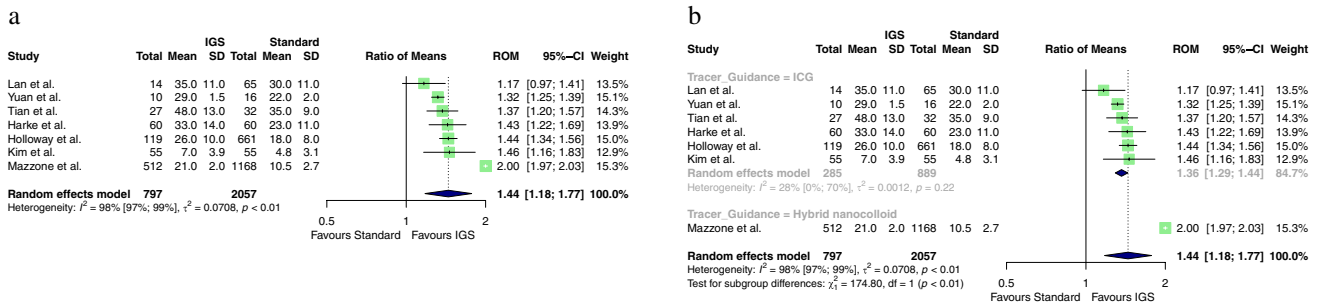


Fig. 5 Quantitative synthesis concerning the number of nodes retrieved, **a** regardless of tracer type; **b** according to tracer type

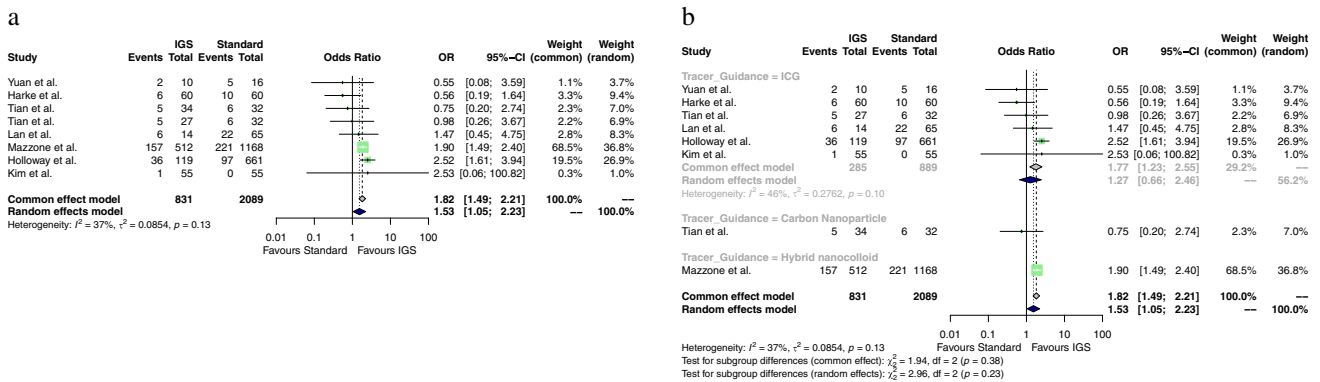


Fig. 6 Quantitative synthesis concerning the rate of metastatic nodal involvement, **a** regardless of tracer type; **b** according to tracer type

perioperative outcomes compared to standard surgery. Notably, these improvements were observed in LOS, EBL, positive surgical margins rate, number of nodes retrieved, rate of pN1, and renal function deterioration (in the case

of partial nephrectomy). Conversely, no statistically significant difference was found for operative time and perioperative complications. Irrefutable reasons for such observations are currently not available. Nonetheless, from

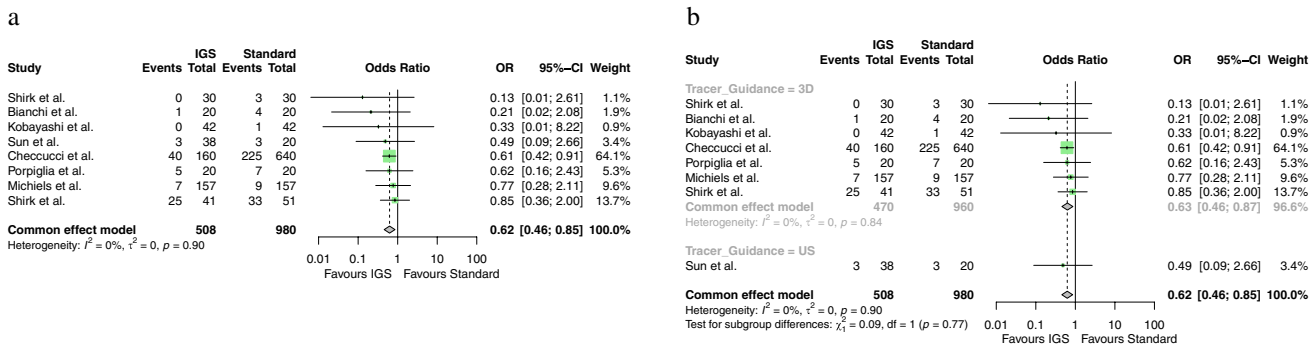


Fig. 7 Quantitative synthesis concerning positive surgical margins, **a** regardless of tracer type; **b** according to tracer type

a surgical standpoint, it is reasonable to hypothesize that the usage of intraoperative guidance might increase the accuracy of a procedure to an extent where the more accurate visualization of the targets, the greater distinction of healthy and malignant tissues, and the more reliable identification of noble structures (e.g., blood vessels, nerves, organs) translate in better overall patient outcomes. Therefore, a clearer view of the surgical field may restrain the blood loss, which can foster the postoperative recovery and decrease the hospitalization time. Similarly, it may provide better oncologic and functional outcomes. For instance, IGS-based selective or super-selective arterial clamping during partial nephrectomy may favorably impact postoperative renal function preservation [18].

These results warrant careful consideration for several reasons. First, the widespread adoption of IGS in recent years underscores its clinical potential [55]. Ensuring the complete removal of tumors without positive margins and preserving healthy tissue is crucial for enhancing patient survival and improving functional outcomes. Therefore, incorporating intraoperative guidance may be essential for surgeons. However, it is undoubtable that the current level of evidence in favor of IGS is limited, and this work provides some proofs of that. It is of note that out of more than 13,000 studies, only three compared a specific IGS vs control, in a randomized controlled fashion [31, 44, 49]. Specifically, these studies only concerned the field of urology, with overall 304 patients being recruited, either

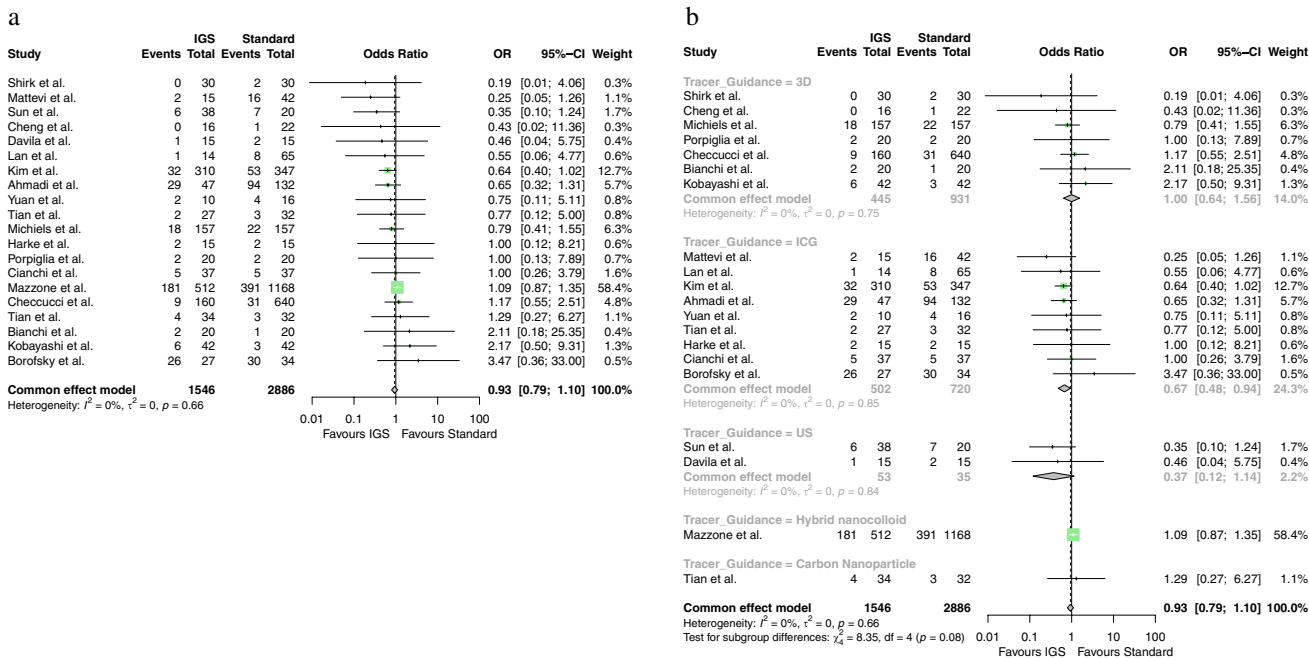


Fig. 8 Quantitative synthesis concerning postoperative complications, **a** regardless of tracer type; **b** according to tracer type

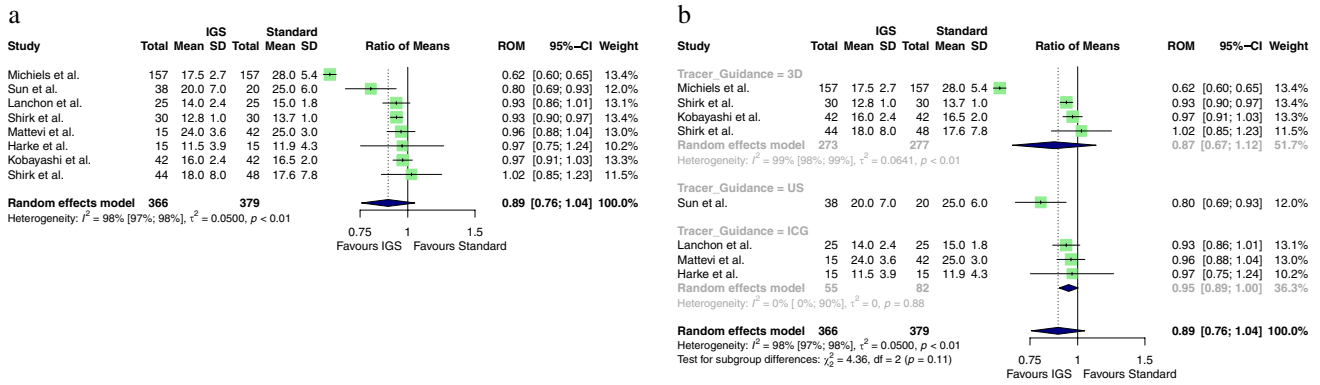


Fig. 9 Quantitative synthesis concerning ischemia time during nephron sparing surgery, **a** regardless of tracer type; **b** according to tracer type

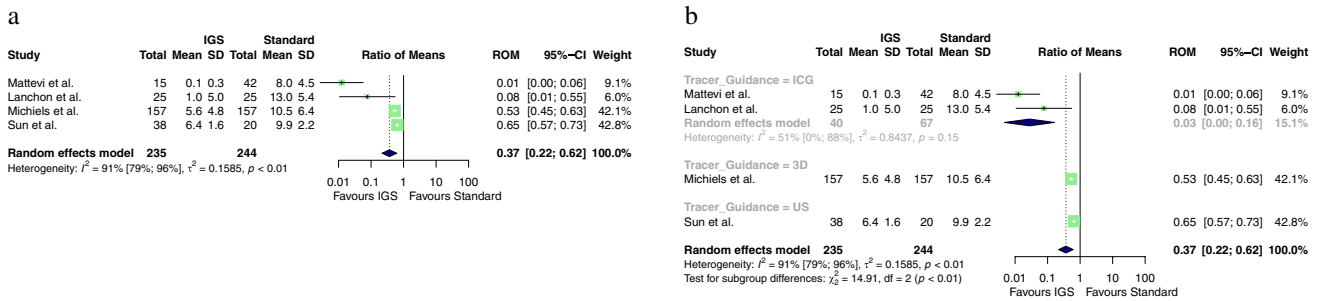


Fig. 10 Quantitative synthesis concerning renal function reduction after nephron sparing surgery, **a** regardless of tracer type; **b** according to tracer type

submitted to partial nephrectomy for kidney cancer or prostatectomy for prostate cancer. Additionally, in all three cases, the outcomes of interest were potential surrogates of cancer-control (e.g., surgical margins, positive lymph nodes), with no mention to overall or cancer-specific survival [31, 44, 49]. Hence, these data are still immature, not easily generalizable, and invariably incapable of demonstrating any certain advantages of IGS implemented to robotic surgery. However, despite the aforementioned limitations, to the best of our knowledge we are the first to undertake the mission to provide the first contemporary systematic review that evaluate the quality of the available literature on IGS in robotic surgery and to assess the potential surgical benefit of the adoption of IGS during robotic procedures across different surgical specialties.

While intraoperative ultrasound is the most commonly used, other imaging techniques such as X-ray, CT, MRI, or nuclear imaging are primarily utilized for surgical planning but are not able to provide real-time intraoperative guidance [56]. Indeed, regarding nuclear imaging, novel drop-in gamma probes can intraoperatively assist the surgeon. However, these lack from image, which may be provided by additional intraoperative tools (e.g., fluorescence) [57, 58]. Therefore, emerging techniques like

NIRF with ICG and 3D/VR guidance are gaining traction in various settings.

Fluorescence imaging relies on a camera capturing light emitted by a fluorescent dye visible when excited with an appropriate light source [56]. These imaging tools can be integrated into laparoscopic or robotic instruments. Various fluorescent contrast agents, typically emitting in the near-infrared region (between 650 and 900 nm), can penetrate several millimeters into tissue [59]. For instance, ICG and methylene blue are two FDA-approved near-infrared fluorophores widely used in numerous surgical applications [60]. In other settings, 5-aminolevulinic acid hexyl ester is employed for malignant gliomas, and non-fluorescent dyes like hexyl ester are widely used for bladder cancer visualization [61, 62]. Over recent years, more specific fluorescent agents have been increasingly used, in particular the use of multimodality imaging [63]. For instance, ^{99m}Tc -nanocolloid associated with ICG is a novel contrast agent implemented across various clinical fields [63, 64]. Another approach involves activatable fluorescent tracers that become visible upon enzymatic cleavage [56]. Other groups are currently evaluating antibodies or fragments labeled with NIRF tracers in preclinical settings, targeting alternative biomarkers for IGS applications [65–69]. Some of these novel molecular biomarkers have been tested in clinical setting into

phase I or II studies [70–75]; on the other hand, RCTs have been planned to test the efficacy on oncological outcomes of integrating molecular targets with intraoperative fluorescence guidance [76]. Similar developments involve small molecules or peptides [60, 77].

Unfortunately, lack of proper structured pipeline for implementing these novel techniques is one the main limiting factor for bridging the gap between the pre-clinical discovery of a novel biomarker or imaging modality and their formal evaluation into clinical practice, thus preventing a timely application after the initial pre-clinical conception. Moreover, other key factors are the technical requirements for surgical manufacturers to adapt and integrate their systems with novel technologies. In this direction, there is an impelling need for a constructive dialogue between researchers and industries with the goal of defining common areas of research and optimizing resources allocation.

Additionally, despite these advancements, the issue of cost–benefit needs to be taken into consideration. The costs associated with novel imaging modalities can be substantial without clear clinical benefits [78]. Unfortunately, accurate discussions on the topic cannot be easily done, based on the paucity of formal cost-analyses [79] and since capital costs, including intraoperative guidance tools, vary widely according to institutional and amortization practices [80]. For instance, as previously reported, the cost of adding NIRF to a robotic system is approximately \$100,000 [81], with a per vial cost of ICG ranging \$80–100 [80, 81]. Therefore, whether the added cost of such technologies is justified may depend on the institution, on the surgeon, and on the expected quality of outcomes without using IGS, as previous authors have already stated [81].

Beyond the challenge of creating new tracers, identifying new potential targets poses a significant hurdle. The ideal biomarker should exhibit high expression in tumors and lower expression in healthy tissue, preferably being extracellular for being targeted by non-penetrating molecules but able to be internalized for a lasting signal. The biomarker should also demonstrate specificity across different types and subtypes of cancers.

Unfortunately, the available data did not permit a specific analysis of individual operations or IGS modalities. The results are generalized to IGS as an innovative surgical approach, integrating state-of-the-art surgery with novel imaging modalities, rather than specifying which imaging modality improves perioperative outcomes in specific surgeries. Thus, each IGS should be evaluated independently before clinical implementation. Moreover, the vast majority of the included comparative studies relied on retrospective data. Therefore, the reported results must be interpreted within the boundaries of such limitation, since selection biases could be operational, and heterogeneity in key factors (e.g.,

inclusion criteria, template of lymph node dissection, surgical technique such as for prostatectomy, partial nephrectomy and pyeloplasty, surgical expertise) could undermine results interpretability. This being said, the risk of bias assessment revealed that the overall quality of evidence in this meta-analysis was moderate, as most studies demonstrated moderate or low risk of bias (Supplementary Fig. 1a–b).

In conclusion, IGS is still in its early stages. Large, multi-center, randomized controlled trials are imperative to determine the benefits of IGS for patients. However, the absence of a general consensus on standardized protocols for the clinical evaluation of new techniques complicates the conduct of multicenter trials and the comparison between clinical studies. Nevertheless, our meta-analysis has demonstrated that the implementation of IGS has the potential to enhance surgical outcomes across various specialties and operations.

Conclusions

The current study suggests that the performance of robot-assisted surgery might be consistently enhanced by intraoperative image guidance. This is especially true when pathologic outcomes are considered. The usage of IGS might increase the detection of metastatic lymph nodes, and simultaneously it can boost the precision of tumor resection, as testified by the significant reduction of positive surgical margins at final pathology. Therefore, IGS has the potential to impact patient prognosis, besides surgical conduct.

Supplementary Information The online version contains supplementary material available at <https://doi.org/10.1007/s00259-024-06706-w>.

Author contribution Conception and design: PDO, EM, ST.

Literature search: ST, FC, AM, FA, RD, AD, EP, AL, ML, MLP, FB, LA.

Title and abstract screening: ST, FC, AM, FA, RD, AD, EP, AL, ML, MLP, FB.

Full text screening: ST, FC, AM, FA, RD, AD, EP, AL, ML, MLP, FB.

Data extraction: ST, FC, EP, LA.

Analysis/interpretation of data: PDO, EM, CAB, GF.

Statistical analysis: PDO, EM, GF.

Drafting the manuscript: ST, GF, FC, EM, PDO.

Critically revising the manuscript: All authors discussed the results and implications and commented on the manuscript at all stages.

Final approval of the manuscript: All authors.

Data availability The code for the analyses will be made available upon request.

Declarations

Ethics consent Study-specific Institutional Review Board ethics approval was not required.

Patient consent statement, permission to reproduce material from other sources and clinical trial registration Not applicable.

Conflict of interest The authors declare no competing interests.

References

- Leal Ghezzi T, Campos Corleta O. 30 years of robotic surgery. *World J Surg* [Internet]. 2016 [cited 2023 Dec 5];40:2550–7. Available from: <https://pubmed.ncbi.nlm.nih.gov/27177648/>
- Brassetti A, Ragusa A, Tedesco F, Prata F, Cacciatore L, Iannuzzi A, et al. Robotic surgery in urology: history from PROBOT® to HUGOTM. *Sensors (Basel)* [Internet]. 2023 [cited 2023 Dec 5];23. Available from: <https://pubmed.ncbi.nlm.nih.gov/37631641/>
- Vidal-Sicart S, Valdés Olmos R, Nieweg OE, Faccini R, Grootendorst MR, Wester HJ, et al. From interventionist imaging to intraoperative guidance: new perspectives by combining advanced tools and navigation with radio-guided surgery. *Rev Esp Med Nucl Imagen Mol* [Internet]. 2018 [cited 2023 Dec 5];37:28–40. Available from: <https://pubmed.ncbi.nlm.nih.gov/28780044/>
- Jackson RS, Schmalbach CE. New frontiers in surgical innovation. *Otolaryngol Clin North Am* [Internet]. 2017 [cited 2023 Dec 5];50:733–46. Available from: <https://pubmed.ncbi.nlm.nih.gov/28601195/>
- Porpiglia F, Amparore D, Checcucci E, Autorino R, Manfredi M, Iannizzi G, et al. Current use of three-dimensional model technology in urology: a road map for personalised surgical planning. *Eur Urol Focus* [Internet]. 2018 [cited 2023 Dec 5];4:652–6. Available from: <https://pubmed.ncbi.nlm.nih.gov/30293946/>
- Ahern DP, Gibbons D, Schroeder GD, Vaccaro AR, Butler JS. Image-guidance, robotics, and the future of spine surgery. *Clin Spine Surg* [Internet]. 2020 [cited 2023 Dec 5];33. Available from: <https://pubmed.ncbi.nlm.nih.gov/31425306/>
- Schols RM, Connell NJ, Stassen LPS. Near-infrared fluorescence imaging for real-time intraoperative anatomical guidance in minimally invasive surgery: a systematic review of the literature. *World J Surg* [Internet]. 2015 [cited 2023 Dec 5];39:1069–79. Available from: <https://pubmed.ncbi.nlm.nih.gov/25522896/>
- Lubner MG, Gettle LM, Kim DH, Ziemlewicz TJ, Dahiya N, Pickhardt P. Diagnostic and procedural intraoperative ultrasound: technique, tips and tricks for optimizing results. *Br J Radiol* [Internet]. 2021 [cited 2023 Dec 5];94. Available from: <https://pubmed.ncbi.nlm.nih.gov/33684305/>
- Checcucci E, Amparore D, Fiori C, Manfredi M, Ivano M, Di Dio M, et al. 3D imaging applications for robotic urologic surgery: an ESUT YAUWP review. *World J Urol* [Internet]. 2020 [cited 2023 Dec 5];38:869–81. Available from: <https://pubmed.ncbi.nlm.nih.gov/31456017/>
- Amparore D, Piramide F, Verri P, Checcucci E, De Cillis S, Piana A, et al. New generation of 3D virtual models with perfusional zones: perioperative assistance for the best pedicle management during robotic partial nephrectomy. *Curr Oncol* [Internet]. 2023 [cited 2023 Dec 5];30:4021–32. Available from: <https://pubmed.ncbi.nlm.nih.gov/37185417/>
- van der Poel HG, Grivas N, van Leeuwen F. Comprehensive assessment of indocyanine green usage: one tracer, multiple urological applications. *Eur Urol Focus* [Internet]. 2018 [cited 2023 Dec 5];4:665–8. Available from: <https://pubmed.ncbi.nlm.nih.gov/30197043/>
- Cacciamani GE, Shakir A, Tafuri A, Gill K, Han J, Ahmadi N, et al. Best practices in near-infrared fluorescence imaging with indocyanine green (NIRF/ICG)-guided robotic urologic surgery: a systematic review-based expert consensus. *World J Urol* [Internet]. 2020 [cited 2023 Dec 5];38:883–96. Available from: <https://pubmed.ncbi.nlm.nih.gov/31286194/>
- Daskalaki D, Aguilera F, Patton K, Giulianotti PC. Fluorescence in robotic surgery. *J Surg Oncol* [Internet]. 2015 [cited 2024 Jan 28];112:250–6. Available from: <https://pubmed.ncbi.nlm.nih.gov/25974861/>
- Beyer LP, Wiggermann P. Planning and guidance: new tools to enhance the human skills in interventional oncology. *Diagn Interv Imaging* [Internet]. 2017 [cited 2024 Jan 28];98:583–8. Available from: <https://pubmed.ncbi.nlm.nih.gov/28818346/>
- van der Poel HG, Grivas N, van Leeuwen F. Comprehensive assessment of indocyanine green usage: one tracer, multiple urological applications. *Eur Urol Focus* [Internet]. 2018 [cited 2024 Jan 28];4:665–8. Available from: <https://pubmed.ncbi.nlm.nih.gov/30197043/>
- PRISMA statement.
- Sterne JA, Hernán MA, Reeves BC, Savović J, Berkman ND, Viswanathan M, et al. ROBINS-I: a tool for assessing risk of bias in non-randomised studies of interventions. *BMJ* [Internet]. 2016 [cited 2023 Dec 5];355. Available from: <https://pubmed.ncbi.nlm.nih.gov/27733354/>
- Lanchon C, Arnoux V, Fiard G, Descotes JL, Rambeaud JJ, Lefrancq JB, et al. Super-selective robot-assisted partial nephrectomy using near-infrared fluorescence versus early-unclamping of the renal artery: results of a prospective matched-pair analysis. *Int Braz J Urol*. 2018;44:53–62.
- Borofsky MS, Gill IS, Hemal AK, Marien TP, Jayaratna I, Krane LS, et al. Near-infrared fluorescence imaging to facilitate super-selective arterial clamping during zero-ischaemia robotic partial nephrectomy. *BJU Int*. 2013;111:604–10.
- Mattevi D, Luciani LG, Mantovani W, Cai T, Chiodini S, Vattovani V, et al. Fluorescence-guided selective arterial clamping during RAPN provides better early functional outcomes based on renal scan compared to standard clamping. *J Robot Surg*. 2019;13:391–6.
- Harke N, Schoen G, Schiefelbein F, Heinrich E. Selective clamping under the usage of near-infrared fluorescence imaging with indocyanine green in robot-assisted partial nephrectomy: a single-surgeon matched-pair study. *World J Urol*. 2014;32:1259–65.
- Ahmadi N, Ashrafi AN, Hartman N, Shakir A, Cacciamani GE, Freitas D, et al. Use of indocyanine green to minimise ureteric strictures after robotic radical cystectomy. *BJU Int*. 2019;124:302–7.
- Grivas N, Wit EMK, Kuusk T, KleinJan GH, Donswijk ML, Van Leeuwen FWB, et al. The impact of adding sentinel node biopsy to extended pelvic lymph node dissection on biochemical recurrence in prostate cancer patients treated with robot-assisted radical prostatectomy. *J Nucl Med*. 2018;59:204–9.
- Harke NN, Godes M, Wagner C, Addali M, Fangmeyer B, Urbanova K, et al. Fluorescence-supported lymphography and extended pelvic lymph node dissection in robot-assisted radical prostatectomy: a prospective, randomized trial. *World J Urol*. 2018;36:1817–23.
- Mazzone E, Dell'Oglio P, Grivas N, Wit E, Donswijk M, Briganti A, et al. Diagnostic value, oncological outcomes and safety profile of image-guided surgery technologies during robot-assisted lymph node dissection with sentinel node biopsy for prostate cancer. *J Nucl Med*. 2021;62.
- Yuan P, Yao K, Zhou Z, Liu J, Li C, Hou W, et al. “Light green up”: indocyanine green fluorescence imaging-guided robotic bilateral inguinal lymphadenectomy by the hypogastric subcutaneous approach for penile cancer. *Eur Urol Open Sci*. 2022;45:1–7.
- Holloway RW, Gupta S, Stavitzki NM, Zhu X, Takimoto EL, Gubbi A, et al. Sentinel lymph node mapping with staging lymphadenectomy for patients with endometrial cancer increases the detection of metastasis. *Gynecol Oncol*. 2016;141:206–10.
- El-Achi V, Burling M, Al-Aker M. Sentinel lymph node biopsy at robotic-assisted hysterectomy for atypical hyperplasia and endometrial cancer. *J Robot Surg*. 2022;16:1111–5.
- Yu HW, Chung JW, Yi JW, Song RY, Lee JH, Kwon H, et al. Intraoperative localization of the parathyroid glands with indocyanine green and Firefly(R) technology during BABA robotic thyroidectomy. *Surg Endosc*. 2017;31:3020–7.
- Ouyang H, Wang B, Sun B, Cong R, Xia F, Li X. Application of indocyanine green angiography in bilateral axillo-breast approach


- robotic thyroidectomy for papillary thyroid cancer. *Front Endocrinol (Lausanne)*. 2022;13.
31. Kim JC, Lee JL, Park SH. Interpretative guidelines and possible indications for indocyanine green fluorescence imaging in robot-assisted sphincter-saving operations. *Dis Colon Rectum*. 2017;60:376–84.
 32. Kim WW, Choi JA, Lee J, Jung JH, Park HY. Fluorescence imaging-guided robotic thyroidectomy and central lymph node dissection. *J Surg Res*. 2018;231:297–303.
 33. Lan YT, Huang KH, Chen PH, Liu CA, Lo SS, Wu CW, et al. A pilot study of lymph node mapping with indocyanine green in robotic gastrectomy for gastric cancer. *SAGE Open Med*. 2017;5.
 34. Cianchi F, Indennitate G, Paoli B, Ortolani M, Lami G, Manetti N, et al. The clinical value of fluorescent lymphography with indocyanine green during robotic surgery for gastric cancer: a matched cohort study. Available from: <https://doi.org/10.1007/s11605-019-04382-y>
 35. Tian Y, Lin Y, Guo H, Hu Y, Li Y, Fan L, et al. Safety and efficacy of carbon nanoparticle suspension injection and indocyanine green tracer-guided lymph node dissection during robotic distal gastrectomy in patients with gastric cancer. *Surg Endosc*. 2022;36:3209–16.
 36. Shirk JD, Kwan L, Saigal C. The use of 3-dimensional, virtual reality models for surgical planning of robotic partial nephrectomy. *Urology*. 2019;125:92–7.
 37. Shirk JD, Thiel DD, Wallen EM, Linehan JM, White WM, Badani KK, et al. Effect of 3-dimensional virtual reality models for surgical planning of robotic-assisted partial nephrectomy on surgical outcomes: a randomized clinical trial. *JAMA Netw Open*. 2019;2.
 38. Kobayashi S, Cho B, Mutaguchi J, Inokuchi J, Tatsugami K, Hashizume M, et al. Surgical navigation improves renal parenchyma volume preservation in robot-assisted partial nephrectomy: a propensity score matched comparative analysis. *J Urol*. 2020;204:149–56.
 39. Michiels C, Khene ZE, Prudhomme T, Boulenger de Hauteclouque A, Cornelis FH, Percot M, et al. 3D-Image guided robotic-assisted partial nephrectomy: a multi-institutional propensity score-matched analysis (UroCCR study 51). *World J Urol*. 2023;41:303–13.
 40. Cheng S, Li X, Zhu W, Li W, Wang J, Yang J, et al. Real-time navigation by three-dimensional virtual reconstruction models in robot-assisted laparoscopic pyeloplasty for ureteropelvic junction obstruction: our initial experience. *Transl Androl Urol*. 2021;10:125–33.
 41. Bianchi L, Chessa F, Angiolini A, Cercenelli L, Lodi S, Bortolani B, et al. The use of augmented reality to guide the intraoperative frozen section during robot-assisted radical prostatectomy. *Eur Urol*. 2021;80:480–8.
 42. Shirk JD, Reiter R, Wallen EM, Pak R, Ahlering T, Badani KK, et al. Effect of 3-dimensional, virtual reality models for surgical planning of robotic prostatectomy on trifecta outcomes: a randomized clinical trial. *J Urol*. 2022;208:618–25.
 43. Checcucci E, Pecoraro A, Amparore D, De Cillis S, Granato S, Volpi G, et al. The impact of 3D models on positive surgical margins after robot-assisted radical prostatectomy. *World J Urol*. 2022;40:2221–9.
 44. Porpiglia F, Checcucci E, Amparore D, Manfredi M, Massa F, Piazzolla P, et al. Three-dimensional elastic augmented-reality robot-assisted radical prostatectomy using hyperaccuracy three-dimensional reconstruction technology: a step further in the identification of capsular involvement. *Eur Urol*. 2019;76:505–14.
 45. Sun Y, Wang W, Zhang Q, Zhao X, Xu L, Guo H. Intraoperative ultrasound: technique and clinical experience in robotic-assisted renal partial nephrectomy for endophytic renal tumors. *Int Urol Nephrol*. 2021;53:455–63.
 46. Davila HH, Abdelhameed S, Malave-Huertas D, Bigay FF, Crawford K, Friedenstab A, et al. Ultrasonography and robotic-assisted laparoscopic sacrocervicopexy with pubocervical fascia reconstruction: comparison with standard technique. *J Robot Surg*. 2020;14:759–66.
 47. Mazzone E, Dell'Oglio P, Grivas N, Wit E, Donswijk M, Briganti A, et al. Diagnostic value, oncologic outcomes, and safety profile of image-guided surgery technologies during robot-assisted lymph node dissection with sentinel node biopsy for prostate cancer. *J Nucl Med [Internet]*. 2021 [cited 2024 Feb 22];62. Available from: <https://pubmed.ncbi.nlm.nih.gov/33547208/>
 48. Friedrich JO, Adhikari NKJ, Beyene J. Ratio of means for analyzing continuous outcomes in meta-analysis performed as well as mean difference methods. *J Clin Epidemiol*. 2011;64:556–64.
 49. Friedrich JO, Adhikari NKJ, Beyene J. The ratio of means method as an alternative to mean differences for analyzing continuous outcome variables in meta-analysis: a simulation study. *BMC Med Res Methodol*. 2008;8:32.
 50. Higgins JPT, Thompson SG, Deeks JJ, Altman DG. Measuring inconsistency in meta-analyses. *BMJ*. 2003;327:557–60.
 51. DerSimonian R, Laird N. Meta-analysis in clinical trials. *Control Clin Trials*. 1986;7:177–88.
 52. Shim SR, Kim SJ. Intervention meta-analysis: application and practice using R software. *Epidemiol Health*. 2019;41: e2019008.
 53. Egger M, Davey Smith G, Schneider M, Minder C. Bias in meta-analysis detected by a simple, graphical test. *BMJ*. 1997;315:629–34.
 54. R: The R Project for Statistical Computing [Internet]. [cited 2022 Apr 14]. Available from: <https://www.r-project.org/>
 55. Mascagni P, Alapatt D, Sestini L, Altieri MS, Madani A, Watanabe Y, et al. Computer vision in surgery: from potential to clinical value. *NPJ Digit Med [Internet]*. 2022 [cited 2023 Dec 5];5. Available from: <https://pubmed.ncbi.nlm.nih.gov/36307544/>
 56. Hernet S, van Manen L, Debie P, Mieog JSD, Vahrmeijer AL. Latest developments in molecular tracers for fluorescence image-guided cancer surgery. *Lancet Oncol [Internet]*. 2019 [cited 2023 Dec 5];20:e354–67. Available from: <https://pubmed.ncbi.nlm.nih.gov/31267970/>
 57. Dell'Oglio P, Meershoek P, Maurer T, Wit EMK, van Leeuwen PJ, van der Poel HG, et al. A DROP-IN gamma probe for robot-assisted radioguided surgery of lymph nodes during radical prostatectomy. *Eur Urol*. 2021;79:124–32.
 58. Dell'Oglio P, de Vries HM, Mazzone E, KleinJan GH, Donswijk ML, van der Poel HG, et al. Hybrid indocyanine green-99mTc-nanocolloid for single-photon emission computed tomography and combined radio- and fluorescence-guided sentinel node biopsy in penile cancer: results of 740 inguinal basins assessed at a single institution. *Eur Urol [Internet]*. 2020 [cited 2024 Jan 28];78:865–72. Available from: <https://pubmed.ncbi.nlm.nih.gov/32950298/>
 59. Gioux S, Choi HS, Frangioni J V. Image-guided surgery using invisible near-infrared light: fundamentals of clinical translation. *Mol Imaging [Internet]*. 2010 [cited 2023 Dec 5];9:237. Available from: <https://pubmed.ncbi.nlm.nih.gov/22583635/>
 60. van Manen L, Handgraaf HJM, Diana M, Dijkstra J, Ishizawa T, Vahrmeijer AL, et al. A practical guide for the use of indocyanine green and methylene blue in fluorescence-guided abdominal surgery. *J Surg Oncol [Internet]*. 2018 [cited 2023 Dec 5];118:283–300. Available from: <https://pubmed.ncbi.nlm.nih.gov/29938401/>
 61. Grossman HB, Stenzl A, Fradet Y, Mynderse LA, Kriegmair M, Witjes JA, et al. Long-term decrease in bladder cancer recurrence with hexaminolevulinate enabled fluorescence cystoscopy. *J Urol [Internet]*. 2012 [cited 2023 Dec 5];188:58–62. Available from: <https://pubmed.ncbi.nlm.nih.gov/22583635/>
 62. Hadjipanayis CG, Widhalm G, Stummer W. What is the surgical benefit of utilizing 5-aminolevulinic acid for fluorescence-guided surgery of malignant gliomas? *Neurosurgery [Internet]*. 2015 [cited 2023 Dec 5];77:663–73. Available from: <https://pubmed.ncbi.nlm.nih.gov/26308630/>

63. Dell'Oglio P, de Vries HM, Mazzone E, KleinJan GH, Donswijk ML, van der Poel HG, et al. Hybrid indocyanine green-99mTc-nanocolloid for single-photon emission computed tomography and combined radio- and fluorescence-guided sentinel node biopsy in penile cancer: results of 740 inguinal basins assessed at a single institution. *Eur Urol* [Internet]. 2020 [cited 2023 Dec 5];78:865–72. Available from: <https://pubmed.ncbi.nlm.nih.gov/32950298/>
64. Fallara G, Pozzi E, Onur Cakir O, Tandogdu Z, Castiglione F, Salonia A, et al. Diagnostic accuracy of dynamic sentinel lymph node biopsy for penile cancer: a systematic review and meta-analysis. *Eur Urol Focus* [Internet]. 2023 [cited 2023 Dec 5];9:500–12. Available from: <https://pubmed.ncbi.nlm.nih.gov/36470729/>
65. Odenthal J, Rijpkema M, Bos D, Wagena E, Croes H, Grenman R, et al. Targeting CD44v6 for fluorescence-guided surgery in head and neck squamous cell carcinoma. *Sci Rep* [Internet]. 2018 [cited 2023 Dec 5];8. Available from: <https://pubmed.ncbi.nlm.nih.gov/29992954/>
66. Boonstra MC, Van Driel PBAA, Keereweer S, Prevoo HAJM, Stammes MA, Baart VM, et al. Preclinical uPAR-targeted multimodal imaging of locoregional oral cancer. *Oral Oncol* [Internet]. 2017 [cited 2023 Dec 5];66:1–8. Available from: <https://pubmed.ncbi.nlm.nih.gov/28249642/>
67. Lwin TM, Miyake K, Murakami T, DeLong JC, Amirfakhri S, Filemoni F, et al. Fluorescent humanized anti-CEA antibody specifically labels metastatic pancreatic cancer in a patient-derived orthotopic xenograft (PDOX) mouse model. *Oncotarget* [Internet]. 2018 [cited 2023 Dec 5];9:37333–42. Available from: <https://pubmed.ncbi.nlm.nih.gov/30647873/>
68. van Driel PBAA, Boonstra MC, Prevoo HAJM, van de Giessen M, Snoeks TJA, Tummers QRJG, et al. EpCAM as multi-tumour target for near-infrared fluorescence guided surgery. *BMC Cancer* [Internet]. 2016 [cited 2023 Dec 5];16. Available from: <https://pubmed.ncbi.nlm.nih.gov/27842504/>
69. Sonn GA, Behesnilian AS, Jiang ZK, Zettlitz KA, Lepin EJ, Bentolila LA, et al. Fluorescent image-guided surgery with an anti-prostate stem cell antigen (PSCA) diabody enables targeted resection of mouse prostate cancer xenografts in real time. *Clin Cancer Res* [Internet]. 2016 [cited 2023 Dec 5];22:1403–12. Available from: <https://pubmed.ncbi.nlm.nih.gov/26490315/>
70. Nishio N, van den Berg NS, van Keulen S, Martin BA, Fakurnejad S, Zhou Q, et al. Optimal dosing strategy for fluorescence-guided surgery with panitumumab-IRDye800CW in head and neck cancer. *Mol Imaging Biol* [Internet]. 2020 [cited 2024 Feb 18];22:156–64. Available from: <https://pubmed.ncbi.nlm.nih.gov/31054001/>
71. Boogerd LSF, Hoogstins CES, Schaap DP, Kusters M, Handgraaf HJM, van der Valk MJM, et al. Safety and effectiveness of SGM-101, a fluorescent antibody targeting carcinoembryonic antigen, for intraoperative detection of colorectal cancer: a dose-escalation pilot study. *Lancet Gastroenterol Hepatol* [Internet]. 2018 [cited 2024 Feb 18];3:181–91. Available from: <https://pubmed.ncbi.nlm.nih.gov/29361435/>
72. Hoogstins CES, Boogerd LSF, Sibinga Mulder BG, Mieog JSD, Swijnenburg RJ, van de Velde CJH, et al. Image-guided surgery in patients with pancreatic cancer: first results of a clinical trial using SGM-101, a novel carcinoembryonic antigen-targeting, near-infrared fluorescent agent. *Ann Surg Oncol* [Internet]. 2018 [cited 2024 Feb 18];25:3350–7. Available from: <https://pubmed.ncbi.nlm.nih.gov/30051369/>
73. Schaap DP, de Valk KS, Deken MM, Meijer RPJ, Burggraaf J, Vahrmeijer AL, et al. Carcinoembryonic antigen-specific, fluorescent image-guided cytoreductive surgery with hyperthermic intraperitoneal chemotherapy for metastatic colorectal cancer. *Br J Surg* [Internet]. 2020 [cited 2024 Feb 18];107:334–7. Available from: <https://pubmed.ncbi.nlm.nih.gov/31960953/>
74. de Gooyer JM, Elekonawo FMK, Bremers AJA, Boerman OC, Aarntzen EHJG, de Reuver PR, et al. Multimodal CEA-targeted fluorescence and radioguided cytoreductive surgery for peritoneal metastases of colorectal origin. *Nat Commun* [Internet]. 2022 [cited 2024 Feb 18];13. Available from: <https://pubmed.ncbi.nlm.nih.gov/35551444/>
75. de Valk KS, Deken MM, Schaap DP, Meijer RP, Boogerd LS, Hoogstins CE, et al. Dose-finding study of a CEA-targeting agent, SGM-101, for intraoperative fluorescence imaging of colorectal cancer. *Ann Surg Oncol* [Internet]. 2021 [cited 2024 Feb 18];28:1832–44. Available from: <https://pubmed.ncbi.nlm.nih.gov/33034788/>
76. Zuur LG, de Barros HA, van Oosterom MN, Berrens A, Donswijk ML, Hendriks JJMA, et al. 99m TcPSMA-radioguided surgery in oligorecurrent prostate cancer: the randomised TRACE-II trial. *BJU Int* [Internet]. 2024 [cited 2024 Feb 18]; Available from: <https://pubmed.ncbi.nlm.nih.gov/38346924/>
77. de Valk KS, Deken MM, Handgraaf HJM, Bhairosingh SS, Bijlstra OD, van Esdonk MJ, et al. First-in-human assessment of cRGD-ZW800–1, a zwitterionic, integrin-targeted, near-infrared fluorescent peptide in colon carcinoma. *Clin Cancer Res* [Internet]. 2020 [cited 2024 Feb 18];26:3990–8. Available from: <https://pubmed.ncbi.nlm.nih.gov/32345649/>
78. Tonutti M, Elson DS, Yang GZ, Darzi AW, Sodergren MH. The role of technology in minimally invasive surgery: state of the art, recent developments and future directions. *Postgrad Med J* [Internet]. 2017 [cited 2023 Dec 5];93:159–67. Available from: <https://pubmed.ncbi.nlm.nih.gov/27879411/>
79. Autorino R, Zargar H, White WM, Novara G, Annino F, Perdonà S, et al. Current applications of near-infrared fluorescence imaging in robotic urologic surgery: a systematic review and critical analysis of the literature. *Urology* [Internet]. 2014 [cited 2024 Jan 28];84:751–9. Available from: <https://pubmed.ncbi.nlm.nih.gov/25260441/>
80. Manny TB, Krane LS, Hemal AK. Indocyanine green cannot predict malignancy in partial nephrectomy: histopathologic correlation with fluorescence pattern in 100 patients. *J Endourol* [Internet]. 2013 [cited 2024 Jan 28];27:918–21. Available from: <https://pubmed.ncbi.nlm.nih.gov/23442199/>
81. Angell JE, Khemees TA, Abaza R. Optimization of near infrared fluorescence tumor localization during robotic partial nephrectomy. *J Urol* [Internet]. 2013 [cited 2024 Jan 28];190:1668–73. Available from: <https://pubmed.ncbi.nlm.nih.gov/23643597/>

Publisher's Note Springer Nature remains neutral with regard to jurisdictional claims in published maps and institutional affiliations.

Springer Nature or its licensor (e.g. a society or other partner) holds exclusive rights to this article under a publishing agreement with the author(s) or other rightsholder(s); author self-archiving of the accepted manuscript version of this article is solely governed by the terms of such publishing agreement and applicable law.

Authors and Affiliations

Stefano Tappero¹ · Giuseppe Fallara² · Francesco Chierigo^{1,3,4,5} · Andrea Micale^{6,7} · Francesca Ambrosini^{4,5} · Raquel Diaz⁵ · Andrea Dorotei^{8,9} · Edoardo Pompeo¹⁰ · Alessia Limena^{11,12} · Carlo Andrea Bravi^{13,14} · Mattia Longoni^{15,16} · Mattia Luca Piccinelli² · Francesco Barletta^{15,16} · Luigi Albano^{10,17} · Elio Mazzone^{15,16} · Paolo Dell'Oglio^{1,18,19} 

✉ Paolo Dell'Oglio
paolo.delloglio@gmail.com

¹ Department of Urology, ASST Grande Ospedale Metropolitano Niguarda, Milan, Italy

² Department of Urology, European Institute of Oncology (IEO), University of Milan, Milan, Italy

³ Department of Urology, Azienda Ospedaliera Nazionale SS. Antonio e Biagio e Cesare Arrigo, Alessandria, Italy

⁴ Department of Urology, IRCCS Ospedale Policlinico San Martino, University of Genova, Genoa, Italy

⁵ Department of Surgical and Diagnostic Integrated Sciences (DISC), University of Genova, Genoa, Italy

⁶ Department of General Surgery, Luigi Sacco University Hospital, Milan, Italy

⁷ Università Degli Studi Di Milano, Milan, Italy

⁸ Department of Orthopaedics, Humanitas Clinical and Research Center, IRCCS, Rozzano, Milan, Italy

⁹ Department of Biomedical Sciences, Humanitas University, Milan, Italy

¹⁰ Neurosurgery and Gamma Knife Radiosurgery Unit, IRCCS Ospedale San Raffaele, Milan, Italy

¹¹ Infertility Unit, Fondazione IRCCS Ca' Granda Ospedale Maggiore Policlinico, Milan, Italy

¹² Department of Clinical Sciences and Community Health, Università degli Studi di Milano, Milan, Italy

¹³ Department of Urology, Northampton General Hospital, Northampton, UK

¹⁴ Department of Urology, Royal Marsden Foundation Trust, London, UK

¹⁵ Unit of Urology/Division of Oncology, Gianfranco Soldera Prostate Cancer Lab, IRCCS San Raffaele Scientific Institute, Milan, Italy

¹⁶ Vita-Salute San Raffaele University, Milan, Italy

¹⁷ Neuroimaging Research Unit, Division of Neuroscience, IRCCS Ospedale San Raffaele, Milan, Italy

¹⁸ Department of Urology, Netherlands Cancer Institute-Antoni Van Leeuwenhoek Hospital, Amsterdam, The Netherlands

¹⁹ Interventional Molecular Imaging Laboratory, Department of Radiology, Leiden University Medical Center, Leiden, The Netherlands